Transmission Design for a Wearable Passive Rehabilitation Device
Bryan Boyer, Rob Shone, Nicholas Skriba, David Stewart

Purpose
We were commissioned to develop and validate mathematical models comparing the relative efficiencies of passive fluid-actuation systems. The purpose of this project is to gain an understanding of the mechanisms driving system efficiency such that a device may be designed for human self-assisted physical stroke-rehabilitation.

This document outlines the background driving our investigation, the various users' requirements we compiled through research, our weighting of these requirements and subsequent development of engineering specifications, and the engineering rationale behind each of the specifications. Additionally, attention is paid towards fluid actuators for their unique characteristics making them particularly attractive for implementation into our proposed passive system. An overview of our mathematical models and testing apparatus is then covered, and the empirical testing results discussed. Finally, we include a discussion section detailing the issues our team faced and future work to be done on this project, in addition to appendices detailing our testing plan, ethical conduct, and extended pneumatic model simulations.

I) PROBLEM DESCRIPTION & CONCEPT GENERATION
Traditionally, physical rehabilitation has been defined as interaction between trained physical therapists and their patients in either hospitals or specialty rehabilitation clinics, and has been dominated by hands-on techniques in which the therapist directly drives the patient's limbs through their range of motion [11]. While this method ensures that the patient receives the desired therapeutic motion, it suffers in the fact that a therapist is required in a 1:1 function for each patient hour of therapy. With the current upward trend in the annual number of strokes [10], the number of individuals requiring specialized rehabilitation will increase in the foreseeable future. Since the majority of individuals are eventually discharged to their homes while continuing physical therapy [8], the implementation of home-based rehabilitation systems has the potential to decrease costs while increasing the patient's access to therapy. It is generally accepted that increasing the number of therapy hours (therapy dosage) has a positive impact on recovery of function [11].

Currently, the promise exists for the paradigm to shift with the invention of many novel rehabilitation devices that provide a range of functionality and breadth of therapy unheard of twenty years ago [11]. While automated therapy has the potential to increase a patient's exposure to rehabilitation activity, two major hindrances still remain. The first is that much of this technology is expensive and cumbersome, and has therefore only been adopted at major clinics, sometimes for the dual purpose of care and research [11]. The second is that most of the devices found on the market rely on complicated electronics [7]. To simplify both the control and the design of the system there is a large advantage in relying on the human body for both actuation as well as control of the system. To date, a purely mechanical system designed around human body power is unknown to exist, largely due to weight and efficiency restrictions found in current production equipment. Of special interest is the potential that fluid power carries, with features arising from its route-ability, high torque-density, valve-ability, and low weight.

1.1 Generation of User Requirements and Engineering Specifications
We began developing our problem statement and project scope after interviewing our team's sponsor and reviewing the desires and requirements divulged. Coupling these requirements with requirements obtained through our research, and the requirements resulting from our ME450 senior design class, we generated a list. Giving each team member a possible 75 weighting points, we then individually weighed each of the requirements with a score of 1-3 as shown in Table 1.

1.2 Generation of Engineering Specifications
After weighing the user requirements we took the top cumulative results and developed engineering specifications around them. The overarching focus of the project was to create a maximum efficiency, minimum loss, high response, and low profile system to transfer mechanical power from one point to another without an intermediary power source. The system has to be flexible and allow the input and output points to move relative to each other independent of the power being transferred. The method by which this transmission works is left up to us, and with each method, the source of loss changes.

Table 1: Generated user requirements and associated engineering specs and rationale.

Requirement	Origin	Weight/12	Engineering Spec.	Rationale
Efficient	Sponsor	12	>80%	Disney Efficiency >80%
Fluid vs. Cable	Sponsor	11	Benchmark Comparison	Compare Efficiencies of Both
Proof of Concept	Sponsor	11	A Functioning Prototype	Sponsor Requirement
Safety	Patient	9	N/A	N/A
Manufacturability	ME450	11	All Machining In-House	Time & Budget Restrictions
Cost	ME450	10	Total Cost $\leq$ $400	ME450 Course Budget
Adjustable	Sponsor	12	Variables Modifiable	Develop Efficiency Transfer Function
Multiple Transmissions	Sponsor	12	Consistent Input-Output	Directly Compare Transmissions
Accurate	Team 16	12	Total Error < 5%	Assessing High Efficiency
Repeatable	Team 16	12	Total Error < 5%	Assessing High Efficiency

We define the mechanical efficiency of our system as the ratio of final system energy to initial system energy, with losses being quantified by the difference between them. Since there can be no power source in between the input and output, the maximum power efficiency is 100%, and the lowest loss is 0%. For fluid systems, losses arise from fluid-dynamic friction at openings and along sidewalls of tubes, mechanical friction at contact points, and thermodynamic damping associated with compressive volume changes in pneumatic systems. Purely Mechanical systems such as Bowden cables suffer from high internal friction within guide-tubes along with contact friction, but do not suffer from the same thermodynamic damping found in fluid systems.

We define responsiveness as the settling time of the output displacement response for a given input. This has a direct correlation with the compressibility of the substance being used since elastic strain energy is stored in material compression. Materials with lower compressibility store less energy in latent pressure, and are therefore able to transfer more energy directly to the system output. The Profile of the system is seen as the average cross-sectional area from the input to the output. Changing the length of the device does not have an impact on the average area.

The various methods power transmission methods have many associated tradeoffs between efficiency, responsiveness, and weight that we must consider for our design. Cable systems, while relatively stiff in axial tension, suffer from frictional losses resulting from conduit-cable surface contact that is a function of length, bend radius, and pretension [1]. Hydraulic systems also remain relatively stiff in the axial direction, yet suffer similar types off frictional losses arising from viscous friction within conduit tubing between actuators. Additionally, hydraulic cylinders suffer mechanical losses within the pistons themselves from material contact, and may suffer from leaky fittings and seals that act to degrade the overall efficiency of the system. Pneumatic cylinders may be categorized by many of the same types of losses as hydraulic cylinders since they both function similarly, however when considering pneumatic systems it is important to take thermodynamic effects into account since the working fluid is compressible. The rise in temperature associated with gas compression gives rise to the potential for irreversible heat transfer between the working fluid and the environment [1].

1.3 Overview of Current Market and Research Being Done
The development occurring today in the realms of efficiency, miniaturization, and flexible-actuation are of special interest since the vast majority of fluid system development has been focused on systems containing 'infinite' power sources (i.e. compressor driven). These advances have been applied to biological and bio-inspired systems and show a promising trend towards future implementation into a completely passive, human body controlled device.

1.3.a Efficiency
Advances in the efficiency of fluid systems dates back decades with the advent of various piston sealing mechanisms (i.e. ring, gap, and rolling diaphragm), and also with experimentation into the minimization of elastic losses in pneumatic systems [5]. The recent application of these principles by Disney Research to a completely passive system [12] shows great promise for implementation into a 'self-assist' rehabilitation device. While

tradeoffs continue to exist between efficiency, weight, system response dynamics, size, and many other variables, the demonstration of a fluid system with efficiency >80% [12] is proof that high-efficiency is obtainable with hydraulics.

1.3.b Miniaturization

In our research, we found a paper by W. Durfee and J. Xia that investigated small-scale hydraulics and compared them to an equivalent electromechanical system using various measures of efficiency [13]. Their study found that the overall efficiency of the cylinders will increase with an increase in bore size. However, as size is a constraint, there is a limit to how much we will be able to increase efficiency in this manner. They also found that for a hydraulic system to match the output of an electromechanical system while remaining lighter than it, high pressures are required. The study also indicates that the weight required to hit a particular power output can increase significantly as the transmission line is lengthened. Should we decide to use a hydraulic actuation system, we would seek to minimize the amount of tubing in order to increase the weight efficiency. In another paper by the same researchers, they modeled the performance of hydraulic cylinders with various combinations of seals [14]. For configurations in which a piston or rod seal was not utilized, the model was run with clearance gaps of 10μm and 20μm. The most effective configuration for the 10μm clearance was one without seals on either the rod or piston; however, this presents a practical problem, as the lack of seal on the rod could result in leakage of the hydraulic fluid, despite the close fit. The addition of a rod seal eliminates this problem, while resulting in only a small decrease in efficiency for the cylinder sizes we are considering. For a 20μm clearance, the setup with only a piston seal was the most effective, but the possibility of leakage is still an issue. The runner-up here is the setup with both piston and rod seals, the type most commonly seen in use, for which the decrease in efficiency is noticeable, but not significant.

1.3.c Flexibility

Since the development of the bellows and the McKibben Air-Muscle, flexible fluid actuators have been implemented in many applications requiring a high force/weight ratio, mis/changing alignment between actuation points, or complicated actuator shapes. While primarily used in pneumatic applications (i.e. Air-Muscles, air suspensions, air bellows), work has been done with liquids [5] which have the distinct advantage over air in that only negligible strain energy is stored in the working fluid. Adaptation to orthotics has been shown by [9] through the use of custom-fabricated bellows and custom-onboard pump along with control circuit in order to deliver elbow orthosis in a compact and novel design. Further investigation into the efficiency of this system would shed light into the tradeoffs associated with miniature bellows' implementation into a completely passive system. Another novel breakthrough was shown by researchers at MIT who developed a hydraulic, swimming fish robot articulated by an adaptation of the Pneu-Nets concept [6] to a more rigid skeleton. Flexible fluid actuators offer

1.4 Concept Generation and Selection Process

In order to shed adequate light on the efficiency requirements of a body-powered rehabilitation device, we believe that it is necessary to benchmark the efficiencies of actuators and transmission systems of similar scale, and to quantify a target efficiency as it relates to the human interaction with the device. In order to accomplish this, our ideal design would allow for quantification of various mechanisms in terms of efficiency and performance, so as to guide continuing engineering efforts. We began the process of generating design concepts by first assessing our list of requirements and engineering specifications and then determining a practical realization of these for an actuator testing apparatus through expansion of the critical design drivers that we determined to be pertinent to our system.

1.4.a Design Drivers and Functional Decomposition

We developed a list of design drivers stemming from our prioritized engineering requirements and subsequently expanded each with a list of functional solutions. The main drivers we concerned ourselves with dealt with the application of system inputs, the overall system capability, the ease of variability, and the apparatus's overall cost and manufacturability. We then decomposed each of these design drivers into various component functions.

Expanding upon each of these functions, we then individually and collectively generated a list of potential solutions with some overlap and contradiction between competing design drivers, such as in the cases of adjustability and rigidity. Much of the lower-level functions such as protection, weight reduction, and quick release functionality remain applicable after choosing concepts to meet high level functional requirements. However, their manifestation will evolve as decision making becomes increasingly specific, and therefore we began by addressing concept selection at the highest level. For our testing apparatus the highest level functionality concerned the specific application of system inputs, (force, displacement, and velocity), and the measurement technique that would be employed to track the displacement of key points in our system. Before delving into sub system design we chose to further expand upon these two functionalities with the intent of selecting concepts for both.

1.4.b Description of Classes of Concepts: Application of Controlled Inputs and Position Tracking
To apply force, displacement, and/or velocity inputs to the system we generated five significantly different power transmission concepts: directly attached vertical masses, a spring loaded pulley, masses with a fulcrum, a servo motor and leadscrew combination, and a fluid driven system. Each of the systems has distinct advantages over the other systems, especially when considering the tradeoff between simplicity and the number of types of inputs that that system can impart. Table 2 displays these input systems and their associated method of applying a given force, displacement, or velocity input. Specifically, both the leadscrew and fluid-driven designs have the potential to apply both force as well as velocity inputs with different configurations, whereas the potential energy systems can only apply known forces. In order to prescribe a velocity to one of these systems either a motor or tuned damper would be required, which detracts from their simplicity. Finally, it is important to note that the method of tracking displacement will have a different manifestation when applied in each system's case, and geometric calculations may be required to obtain the desired values.

Table 2: Input system classes and respective method of applying force, displacement or velocity inputs.

Input	Force	Displacement	Velocity
Vertical Masses	Masses	Positive Stop	Tuned Damper
Spring Pulley	Spring Potential	Positive Stop	Motor Driven
Fulcrum	Masses, Moment Arm	Positive Stop	Tuned Damper
Lead Screw	Motor Torque	# Revolutions	Motor Speed
Fluid Driven	Pressure	Volume	Flow Rate

In addition to generating different concepts by which inputs could be applied to our testing rig, four significantly different displacement tracking concepts were generated, namely an encoder, an interferometer, an extensometer, and a high speed camera. Significant tradeoffs between measuring systems exist, including contact and non-contact, the type of motion that can be measured most significantly (linear or rotational), and the relative cost in relation to capability which are shown in Table 2 for the four systems we compared.

Table 3: Measurement systems with contact, type of motion tracked, and relative cost to purchase.

Measurement System	Contact	Motion Tracked	Cost
Encoder	Inertia & Friction	Linear or Rotational	Low
Interferometer	Non-Contact	Linear	High
Extensometer	Deflection/Sliding	Linear or Rotational	Low-Mid
High Speed Camera	Non-Contact	Planar	Mid-High

1.4.c Comparison of Generated Concepts
To select our final design concept we qualitatively compared our generated concepts through an identification of pros and cons relating to our generated concepts for applying system inputs (Table 4), and through a qualitative assessment of the range of capability and cost associated with each displacement measuring system (Table 5).

Table 4: Pros/Cons comparison between our generated types of input systems.

Key Variables	Vertical Masses	Spring Pulley	Fulcrum	Lead Screw	Fluid Driven
Pros	Completely Gravity Driven, Simple	Planar, Can use Encoder Directly	High Mech-Adv, Encoder Directly	Force and Velocity Inputs	Easy to Adapt to Fluid Actuators
Cons	Minor off-axis loads	Slop in Pulley Sys: Input Dynamics	Force Input is Non-Linear	Significant Fabrication Time	Adaptation to Bowden Cables

Table 5: Comparison of displacement measurement systems' relative capability, cost, and implementation time.

Key Variables	Encoder	Interferometer	Extensometer	High Speed Camera
Design/Fab Time	Design Data Aq.	Setup and Calibrate	Design Data Aq.	Setup and Calibrate
Cost	~$5-50	>$1000	~ $100-200	Borrow
Accuracy	~ 1 Count	~Micron	0.001 – 0.1 mm	Function of Field of View
Resolution	~1024	Lambda/4 – Lambda/2	0.0001-0.01 mm	Function of Field of View
Repeatability	~ 1 Count	~Micron	0.001 – 0.1 mm	+/- 1 Subpixel

1.5 Final Concept Description

Through our concept generation and selection process we chose to compare the efficiency of several passive power transmission actuators, namely Bowden cables and pneumatic and hydraulic cylinders, aligned in a vertical orientation such that gravity acting on affixed masses would deliver a constant and known input force. Our proposed testing system will track the relative displacements of the input and output actuators in time using rotary optical encoders since they have relatively low uncertainty while remaining cost effective and simple to implement. Since each transmission system's efficiency is a function of a multitude of input variables, and because each class of actuator is dependent on a unique set of variables, the testing apparatus will allow for variation of the most critical parameters in order to validate each one's direct influence on the overall efficiency of each transmission system. By varying the key parameters we hope to gather enough data to validate our simplest competent mathematical models that have been developed for each class of actuator.

In parallel with the development of our testing apparatus, mathematical models are currently under development for each actuator type comprised of the simplest collection of variables that we believe necessary to accurately approximate each class of actuator's overall efficiency. While empirical testing is quite beneficial, we hope to gain a greater understanding of the relationship between each critical parameter and the overall efficiency of the system, and a mathematical model will allow us to quickly simulate the system response with a simple numerical change of any one of the parameters. The benefit of such models is quickly understood as the practical limit of empirical testing is reached rather abruptly when time and budget constraints are taken into consideration. We hope to validate our mathematical models at specific test points which will then allow us to search for an optimal solution through simulation instead of purely empirical testing. The added benefit of potentially obtaining a custom solution is also realized through a mathematical model, because empirical testing is most efficiently done with the use of off-the-shelf components, which may or may not satisfy our high efficiency requirements. Through optimization schemes a mathematical model may point us to such a solution which would then potentially be developed for further testing.

II) MATHEMATICAL MODELING

Our design concept remains somewhat unique amongst the aggregate of projects in that one of our major deliverables is our validated mathematical model. To accomplish this we are developing both our model and testing apparatus in parallel in an effort to quantify the breadth of critical test variables such that the dynamic response of the test system can be directly compared for any combination of input variables in our simulation.

2.1 Bowden Cable Model

Through our research into modeling Bowden cables we discovered research done by a team investigating the effects of conduit geometry on torque and displacement transmission using a master-slave actuator setup [1]. According to their results, the system pretension, cable length, and the conduit spatial profile all contribute to

both torque and displacement transmission between the master and slave units. From their research it is evident that the overall system efficiency is very highly dependent these three factors, Figures 1, 2, and 3 [1].
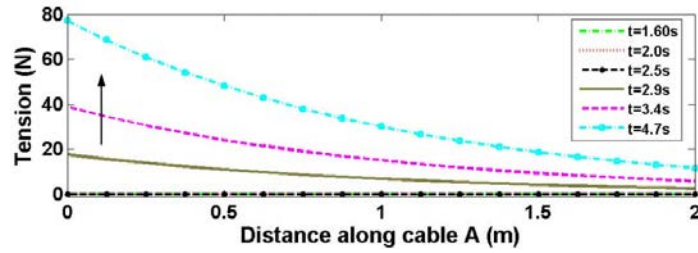

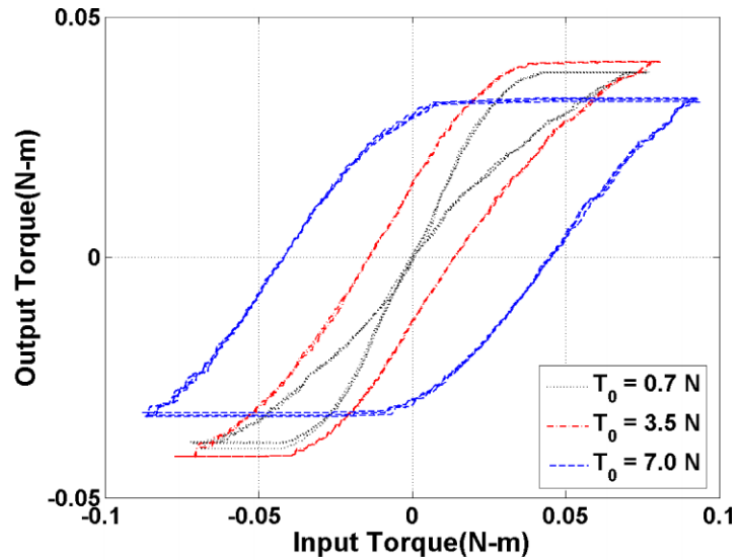Figure 1: Cable tension decay along straight length of cable.

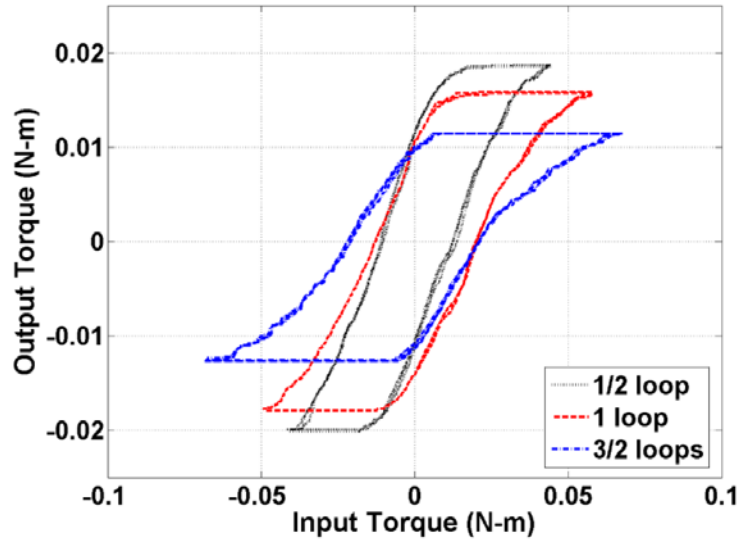Figure 2: Input vs. output torque for different preloading conditions (T_0).

Figure 3: Input vs. output torque through varying numbers of conduit loops.

In order to implement Bowden cables as a practical transmission system the overall system length would need to be minimized, while maintaining the straightest cable geometry possible. Additionally the pretension would need to be optimized since there is a tradeoff between pretension, cable slack, and friction [1].

For our testing we will test Bowden cables at a length that is realistic for human implementation and directly compare the results against pneumatic and hydraulic systems of the same length in order to assess their relative efficiency on the human scale. By adjusting the total enclosure provided by the conduit (Figure 4) and allowing the cable to freely pass between two sections of conduit we believe that the total friction losses can be greatly mitigated, however the extent to which this would have an effect is currently unknown. At this point we have not developed a mathematical model for the cable system, however we are planning on developing a similar model to the one outlined in [1] with the added provision for cable passing through air between two sections of conduit.
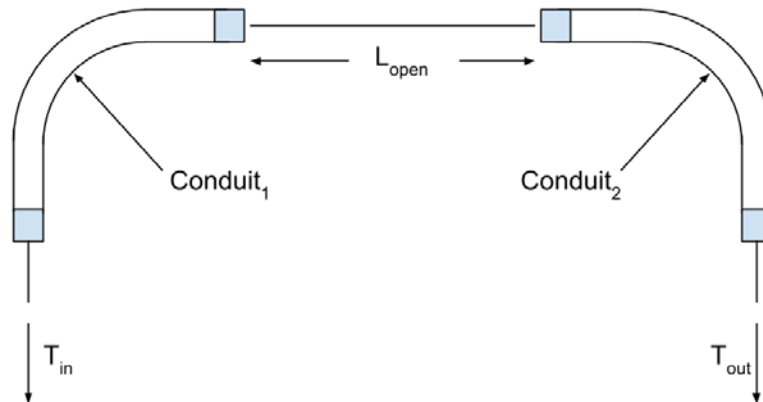
Figure 4: Reduction in overall Bowden cable system friction by removing straight sections of conduit.

2.2 Pneumatic Cylinder Mathematical Model
The efficiency of pneumatic cylinders is significantly more complex than that of Bowden cables since both mechanical and thermodynamic effects must be taken into consideration when developing a mathematical model to evaluate them with. Through our research into the topic it was apparent that pneumatic cylinders acting in a master-slave relationship is somewhat of a novel idea and while research has been done into individual cylinder thermodynamics and friction response, a complete model was not found. We began the development of pneumatic cylinder model by looking into the primary difference between pneumatic and hydraulic actuators, which we identified to be the working fluid's compressibility. Regarding cylinder efficiency, gas compressibility poses two significant challenges arising from energy transfer mechanisms that work to degrade the system's overall capability to do useful work on the environment. The first significant challenge to overcome is the fact that, for given geometric and gas conditions, an applied input force will do work on the control volume of gas to compress it as depicted in Figure 5. Similar to a spring, some of the work done on the control volume is not directly transferred to the output but instead stored as potential energy in the gas control volume. Additionally, compressing a gas results in a rise in the gas' temperature which gives rise to the potential for heat exchange between the gas control volume and the environment (Fig. 5).
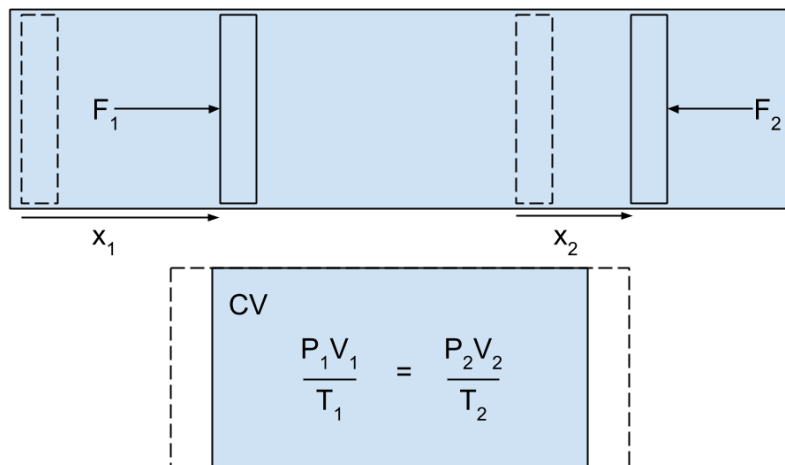

Figure 5: Gas control volume analysis used to evaluate the states of ideal gas within cylinders.

While the efficiency of isentropic compression approaches 100%, pneumatic cylinders in real engineering situations suffer from thermodynamic losses which are a function of the timescale involved and the relative operating conditions [4]. Quickly compressing and expanding the gas inside a cylinder is often times accurately approximated as adiabatic since the relative time scale of actuation is so much shorter than the time required for significant heat transfer. Since our transmission will be implemented in a novel self-assist rehabilitation device where the rate of actuation is not currently understood, we believed it pertinent to incorporate the losses associated with time-dependent heat transfer into our model in an effort to capture the dynamic response of the system. Furthermore, the steady-state error resulting from compression-related displacement losses will also be taken into account when computing the overall pneumatic system efficiency. By treating air as an ideal gas and with the assumption that the cylinder walls are sufficiently thin such that the inside wall temperature can be approximated equal to the ambient temperature, we obtain an equation for the temporal temperature gradient Equation 1 where tau must be obtained experimentally [3], where T_0 and T_g are the ambient and gas temperatures (K), C_v and R are the gas volume-specific heat and specific gas constant (kJ-kg/K), m_g is the mass of the gas (kg), v_{dot} is the time rate of change of the gas' specific volume (m^3/kg-s), A_{wall} is the exposed cylinder wall area (m^2), and *lambda*$_{convection}$ is the average heat transfer coefficient between the air and environment (kW/m^2-K).

$$\dot{T} = = \frac{(T_0 - T_g)}{\tau} - \frac{T_g}{C_v}\left(\frac{dP}{dT}\right)_v \dot{v} \qquad \tau = \frac{m_g C_v}{\lambda_{convect} A_{wall}} \qquad \frac{dP}{dT} = \frac{m_g R}{T} \qquad (1)$$

Since the overall heat transfer is a function of the piston displacement through the surface area of the interior wall, as well as the gas' temperature and pressure through the dependence of the heat transfer coefficient we, propose using a method similar to that outlined in [3] to compute an average convection heat transfer coefficient experimentally for each cylinder and then solve Equation 2 analytically using Matlab's ODE45 solver. Tau must first be determined experimentally as the thermal time constant of the system (s) and then used with initial and average temperature conditions to determine lambda$_0$. Lambda$_0$ can then be used with the dynamic system model to calculate the instantaneous average heat transfer coefficient lambda.

$$\lambda(P,T) = \lambda_0 \left(\frac{PT}{P_0 T_0}\right)^{.5} \qquad \lambda_0 = \lambda_{ave}\left(\frac{P_0 T_0}{P_{ave} T_{ave}}\right)^{.5} \qquad \lambda_{ave} = \frac{m_g C_v}{\tau A_{wall}} \qquad (2)$$

In addition to thermodynamic losses, pneumatic cylinders suffer from mechanical losses arising from complex frictional mechanisms present in the material interaction of the fluid, piston, and barrel. Viscous boundary layer losses in the barrel and transmission lines, and complex flow-restriction head-losses at orifices contribute to very complicated flow losses. While contributing factors, we believe that their contribution to the overall system friction is negligible since the viscosity of air is so low, in comparison to the contact friction between the piston and barrel, and the piston rod and guide bushing. Additionally, since the Mach numbers involved in the proposed rehabilitation device can be assumed to be relatively low (Equation 3), we believe that the pressures in both chambers can be assumed to be equal at any given instant in time. Through these assumptions we will consider air through a lumped parameter control volume analysis with spatial pressure and temperature gradients of zero.

$$M = \frac{v_{tube}}{c} \qquad v_{tube} = v_{input}\frac{A_{cyl}}{A_{tube}} \qquad (3)$$

Even with these assumption the overall mechanical friction can be quite different from cylinder to cylinder based on the type of seals used, whether gap, rolling diaphragm, or contact, as well as whether or not the piston rod is itself sealed. According to [2] the viscous friction response between cylinders can vary as much as 10 (N-s/m) to 667 (N-s/m), and additionally the overall friction of pneumatic cylinders is a function of pressure, piston velocity, as well as geometry, as modeled with the Modified LuGre friction model; in order to compute this friction model, several parameters must be experimentally computed. While the LuGre model is extensively used as a friction modelling technique for servo-control applications, we believe that a simplified model will capture the most significant dynamics, namely static friction and viscous damping. Additionally, both of these can be easily obtained through simple mass-gravity related experiments and do not require a motor-controlled input.

8

Coupling the thermodynamic and mechanical systems together we have developed a simplest competent model for pneumatic cylinders which can be simulated under our testing rig conditions in order to obtain a dynamic response of the system (Figure 6). Shown in Figure 6 and Equations 4-9 are our cylinder model and the associated state-variables used with Matlab's ODE45 solver to simulate the dynamic response of the system for a given vector of input parameters, and set initial conditions. Parameters in the state equations correspond to Figure 6, in addition to *lambda₁* and *lambda₂* which correspond to the average heat transfer coefficients (W/m²-K) for each gas as defined in Eq. 2. The state equations were obtained using Newtonian mechanics and lumped parameter analysis of the total piston masses, in addition to the aforementioned heat transfer relationships.
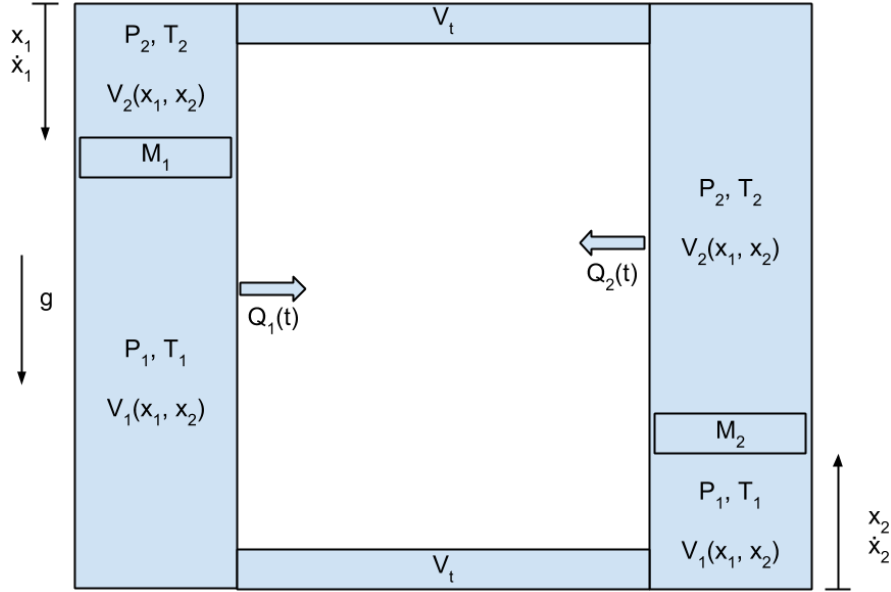
Figure 6: Simplest competent dynamic model for master-slave pneumatic cylinder configuration.

$$\dot{z}_1 = z_2 \tag{4}$$

$$\dot{z}_2 = \frac{1}{m_1}(m_1 g + (P_2 - P_1)A_1 - b_1 \dot{x}_1) \tag{5}$$

$$\dot{z}_3 = z_4 \tag{6}$$

$$\dot{z}_4 = \frac{1}{m_2}(-m_2 g + (P_1 - P_2)A_2 - b_2 \dot{x}_2) \tag{7}$$

$$\dot{z}_5 = (T_0 - T_1)\left(\frac{\lambda_1 A_{wall1}}{m_{g1} C_v}\right) - \frac{T_1}{C_v}\left(\frac{m_{g1} R}{V_1}\right)_v \dot{V}_1 \tag{8}$$

$$\dot{z}_6 = (T_0 - T_2)\left(\frac{\lambda_2 A_{wall2}}{m_{g2} C_v}\right) - \frac{T_2}{C_v}\left(\frac{m_{g2} R}{V_2}\right)_v \dot{V}_2 \tag{9}$$

We consider the preliminary results from our model as reasonable through qualitative analysis of all six state variables and the overall dynamic response of the system as shown by Figure 7. As we would expect, a significant amount of compressive work is done on the control volume of air and is unable to be directly converted into usable mechanical work.
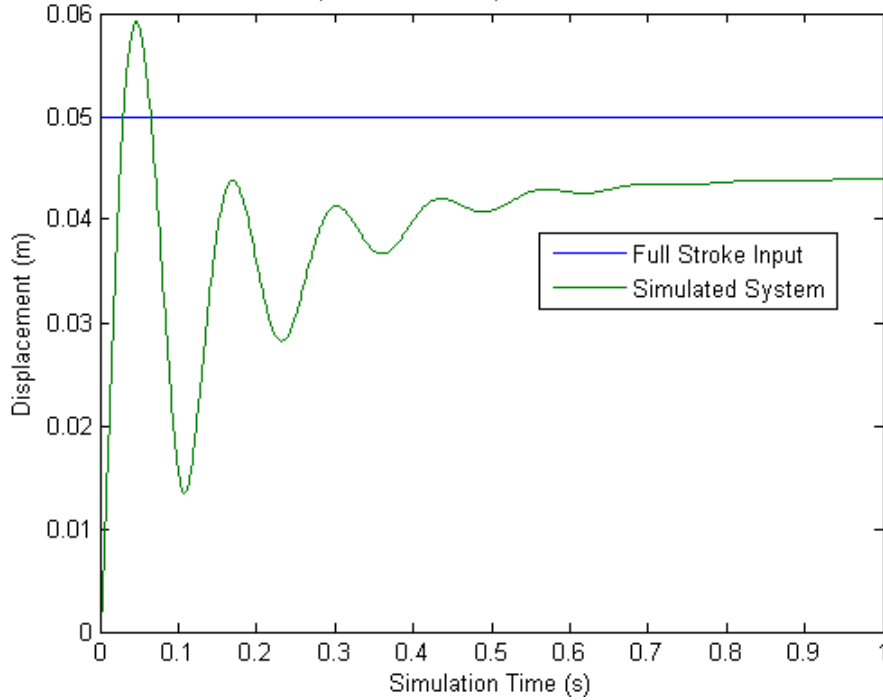
Figure 7: Simulated step response of the system to a full stroke displacement input of 0.050 (m).

The full dynamic response of the system when subjected to gravitational loads is also very interesting since it will provide us a direct comparison to the data we collect during our testing. Shown in Figure 8 is the dynamic response of the same system under a step force input instead of a step displacement input comparing the idealized case (without any mechanical or thermodynamic losses) and the simulated case with losses. The coupled dynamics between the masses show values that appear to be reasonable without any empirical testing, and we are currently in the process of better understanding the total system efficiency resulting from this simulation. Figure 8 shows both the presence of damping as well as a DC offset from the ideal case. Additional simulation results may be found in Appendix 3.
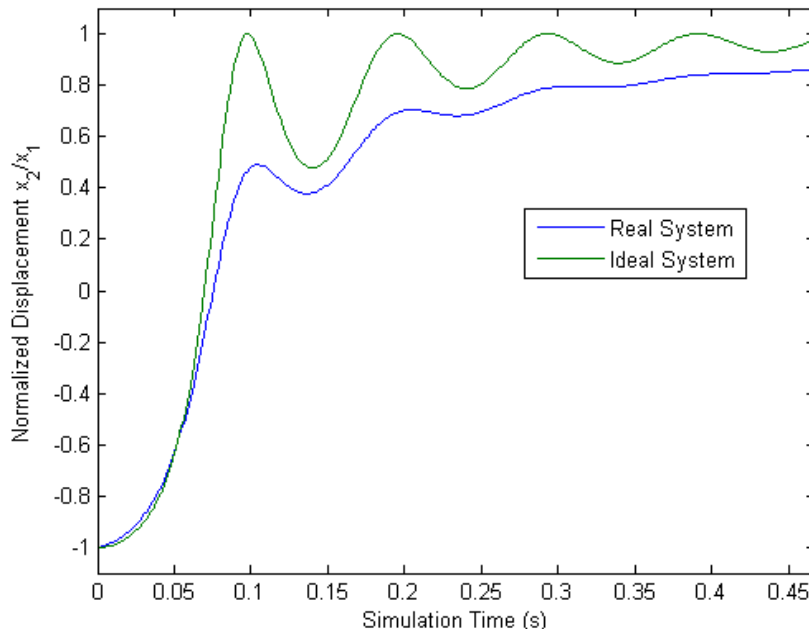

Figure 8: Simulated dynamic tracking response of our system to a step force input.

2.3 Hydraulic Cylinder Mathematical Model

To evaluate the theoretical efficiency of hydraulic actuators, we utilized a model developed by William Durfee and Jicheng Xia of the University of Minnesota [14]. The model defines the overall cylinder efficiency, η, as the product of the force efficiency, η_f, and volumetric efficiency, η_v, which can be further simplified, as shown in Eq. 1. Parameters used in the model are listed in Table 6 and the methods used to calculate Q_a and F_{ar} are shown in Equations 10-18. A detailed derivation of the model can be found in the above-mentioned paper.

$$N = N_f N_v = \frac{F_{ar} U_{ar}}{P Q_a} \tag{10}$$

$$F_{ar} = F_{ir} - f \tag{11}$$

$$Q_a = Q_i + q \tag{12}$$

$$F_{ir} = 0.25\pi B^2 P \tag{13}$$

$$Q_i = 0.25\pi B^2 U_{ar} \tag{14}$$

$$f_{unsealed} = -0.5\pi\delta P D_p + \frac{\pi\mu U_{ar} D_p l}{\delta} + 4\pi\sqrt{\mu * U_{ar}} D_r dE\epsilon\sqrt{2\epsilon - \epsilon^2} \tag{15}$$

$$f_{sealed} = 12650\pi\sqrt{\frac{\mu U_{ar}}{P}} BdE\epsilon\sqrt{2\epsilon - \epsilon^2} + 4\pi\sqrt{\mu U_{ar}} D_r dE\epsilon\sqrt{2\epsilon - \epsilon^2} \tag{16}$$

$$q_{unsealed} = \frac{\pi P D_p \delta^3}{12\mu l} + 0.5\pi U_{ar}\delta D_p \tag{17}$$

$$q_{sealed} = 1.495\pi\mu^{.71} U_{ar}^{1.71}\sigma_m^{-.71} s^{.29} \tag{18}$$

Table 6: Tabulation of parameters used in Durfee hydraulic cylinder efficiency model.

Parameter	Description	(Units)
U_{ar}	Actual rod velocity	m/s
P	Operating pressure	Pa
Q_a	Actual flow rate	m³/s
Q_i	Ideal flow rate	m³/s
F_{ar}	Actual rod force	N
F_{ir}	Ideal rod force	N
f	Friction force	N
B	Bore	m
δ	Clearance gap size	m
D_p	Piston diameter	m
μ	Fluid viscosity	Pa·s
l	Thickness of piston head	m
D_r	Rod diameter	m
d	O-ring cross section diameter	m
E	O-ring Young's modulus	Pa
σ_m	Max O-ring contact pressure	Pa
s	O-ring contact width	m

The model was implemented in Microsoft Excel to enable us to quickly change variables, although a Matlab implementation would allow for more detailed analysis.

2.3.a Preliminary model evaluation

To verify that the model was implemented correctly, we ran two test cases, holding the geometric dimensions of the cylinder, the physical properties of the O-ring, and the rod velocity as constant parameters. The geometry used was that of one of our test cylinders, the Airpel E16DU, the O-ring properties used were the nominal values used in the paper, and the rod velocity was set to 0.01 m/s, which is reasonable for the eventual application of the cylinders. The remaining two parameters, operating pressure and fluid viscosity, were used as variables for this assessment.
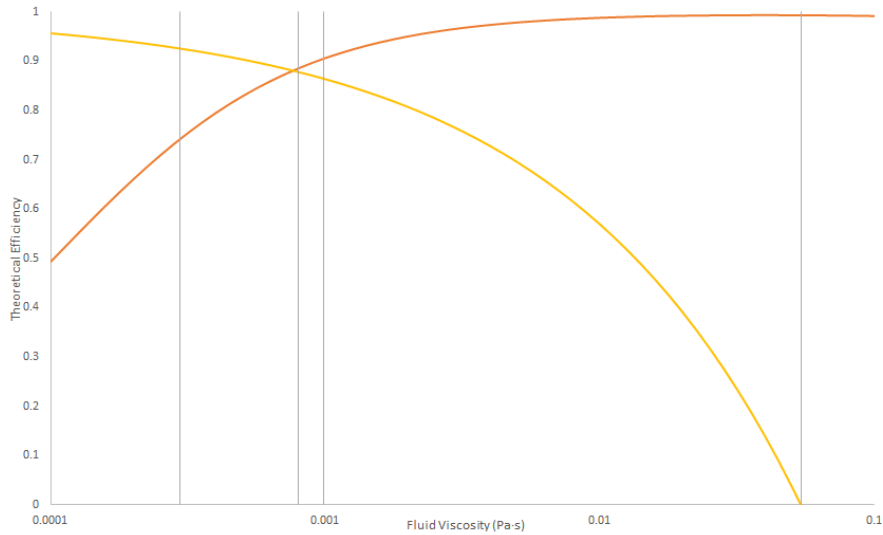
Figure. 9: Theoretical cylinder efficiency vs. fluid viscosity at an operating pressure of 1 (atm). The orange line represents the clearance gap cylinder and the yellow line represents the O-ring sealed cylinder. The grey lines represent viscosities of various fluids and are provided for context (From left: acetone, water, ethanol, olive oil)
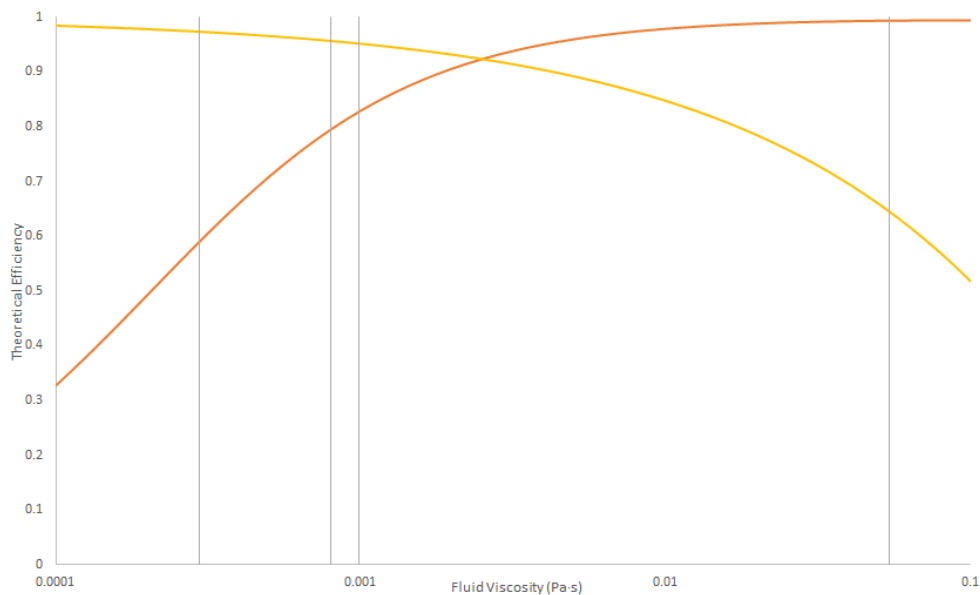

Figure 10: Theoretical efficiency vs. fluid viscosity at an operating pressure of 2 (atm). The orange line represents the clearance gap cylinder and the yellow line represents the O-ring sealed cylinder. The grey lines represent viscosities of various fluids and are provided for context (From left: acetone, water, ethanol, olive oil)

Two cases were evaluated, one operating at 1 (atm) of pressure, Fig 9, and the other at 2 (atm), Fig 10. The viscosity was varied to show the expected change in cylinder efficiency as that variable changed. The efficiency of cylinders with a sealed piston appear to decrease with increased viscosity, whereas the efficiency of clearance gap cylinders increases with increased viscosity. The change in pressure did not change this trend; however, it did increase the range of viscosities in which the sealed cylinder could be reasonably expected to outperform a clearance gap cylinder of the same dimensions. We also found similar interdependence between other parameters and how they affect the efficiency. Pressure and viscosity are likely to be the most feasible to vary in our testing, as we can easily change the working fluid and can pre-pressurize the system to a point of our choosing.

12

2.3.b Model Update

In order to better understand the mathematical model that we seek to validate for hydraulic cylinders [14], we implemented the model in the computational software program Wolfram Mathematica, using the software's 'Manipulate' function. This tool lets the user to define functions to plot or otherwise output and then allows them to interact with the function, with the output updating in real-time. In this particular case, we have configured the code so that the model parameters can be varied with sliders and the plots for various cylinder types can be toggled on and off. Figure 11 shows a sample plot of the model output for the four cylinder configuration types described in the source material. Each of the four curves is a function of various input parameters and calculated variables, each of which is also a function of the input parameters. This method of visualization and interaction allows us to better comprehend the effects of different variables on the expected efficiency.
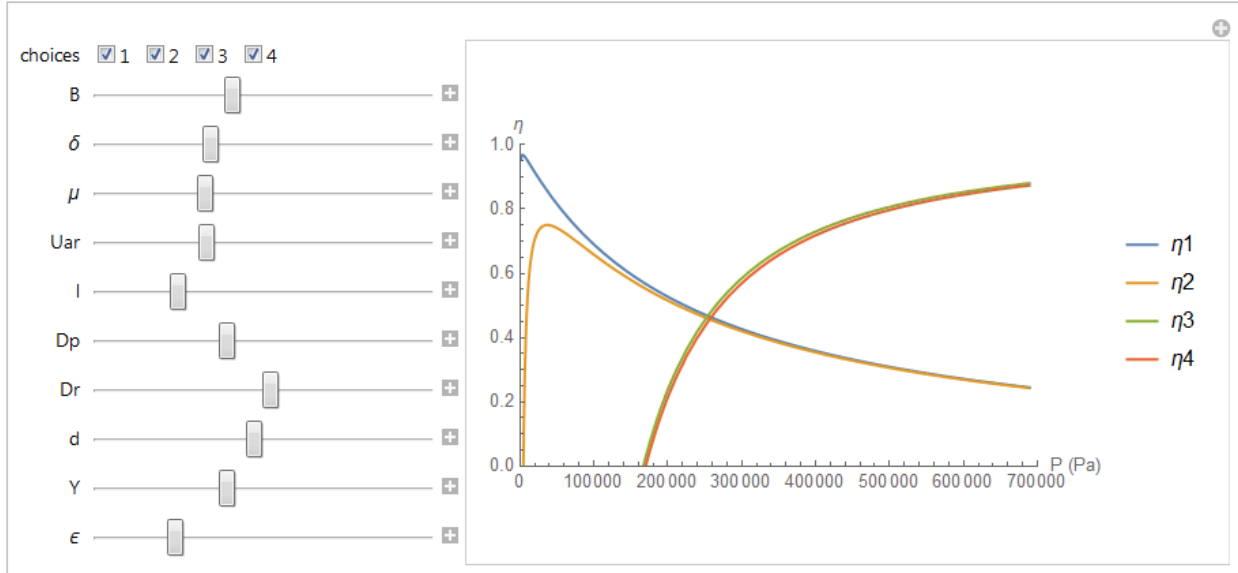

Fig. 11: Graph showing the theoretical efficiencies of four cylinder configurations across a range of operating pressures. The input parameters are defined as in the model. The values used for this sample figure have no particular significance

The current version of the code is functional with regard to its primary purpose of providing an interactive visualization method for the hydraulic model. However, work is still being done to improve the model to improve its usefulness when the time comes for data analysis. In addition to improving the user interface, we are working to provide the ability to display confidence intervals for the efficiency curves to aid in model validation. These intervals are calculated by using uncertainty propagation to determine the impact the uncertainty in each parameter will have on the model as a whole. A test version of the code with this functionality has been completed, but modifications are still being made to enable the user to vary the type of confidence interval, as well as providing the ability to set uncertainties as a percentage of the parameter value, rather than requiring a static value. Future plans for the interactive model include the addition of conduit efficiency and system efficiency, as the proposed transmission system would consist of at least two cylinders and the tubing required to connect them, and a function to allow the plotting of experimental test data overlaying the calculated efficiency curves.

III) EMPIRICAL TESTING

In conjunction with our mathematical model we have begun development of the testing apparatus that will be used to compare the efficiency of different transmissions. To apply known forces to the master and slave actuators we chose to use known masses supported by mass carriages such that gravity acting on the masses applied a known weight.

3.1 Mockup Construction

We developed a simple foam-core mockup of our proposed testing apparatus for Design Review 2 that consisted of two double acting air cylinders connected via tubing in such a way that downward force acting on one cylinder produced an upward displacement in the other cylinder. One key feature of the mockup are the valves and pressure gauge that we plan to use to measure the pre-pressure in the pneumatic and hydraulic systems because our models have shown that pre-pressurizing the system, especially in the pneumatic case, has a positive effect on total system efficiency. The second major function of our mockup is the presence of a Bowden cable conduit which we use to convey the fact that our testing apparatus will be benchmarking cable systems directly against fluid systems. Finally, we placed some proximity sensors at the base of the mockup showing one method of non-contact sensing that we are currently considering.

Figure 12: Foamcore mockup of our proposed test rig incorporating cylinder, a Bowden cable conduit, and sensors.

3.2 Solidworks CAD Model Development

In order to facilitate the manufacturing and assembly process for our testing rig, we developed a CAD model of our proposed design, seen in Figure 12. The rig has support structures on both the top and bottom, which allows the reorientation of the rig for testing single-acting cylinders, as these can be limited in their ability to actuate against vacuum. Actuators will be fixed into place on the adapter plates and connected by flexible tubing (not seen in model). Mass carriages will be rigidly attached to the cylinder rods to allow the use of calibrated masses to actuate motion. On the lower end of the model, we have left room for the implementation of a measurement system.
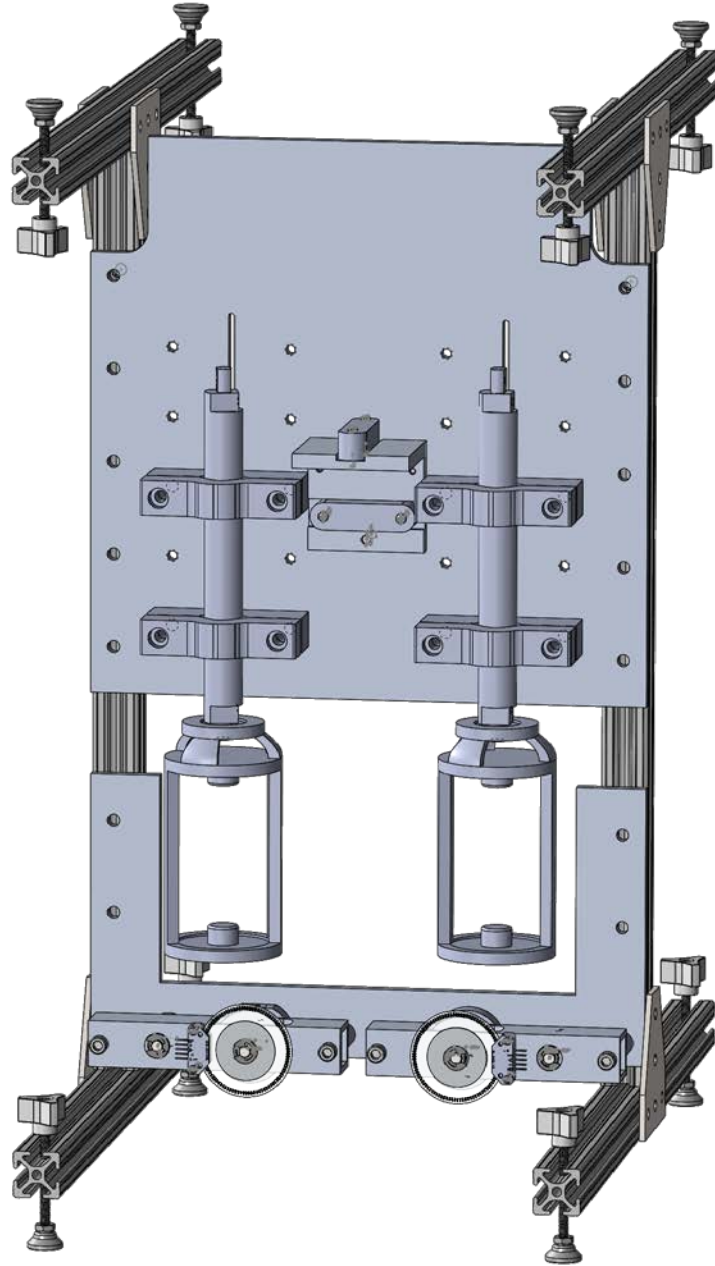
Figure 13: CAD representation of our proposed testing apparatus using Airpel E16D5 cylinders. We note the mass carriages rigidly attached to each cylinder in order to apply a known force, and the system capability to be turned upside down so as to test single acting cylinders.

T-slotted aluminum extrusion with gussets and fasteners were selected to construct the frame and support of the testing rig due to its strength, ease of assembly, and accessibility. The only machining operations necessary for the framing would be cutting the aluminum plate and extrusion to length on the band saw. Any sharp edges can be cleaned up with a file.

3.2.a Testing Apparatus Frame Design
For the frame of our testing apparatus, we chose to use standard 1" t-slotted extrusions for the ease of assembly and structural rigidity. For the 90 degree mounts, 5-screw hole brackets are used in conjunction with the t-slot fasteners (Figure 14).
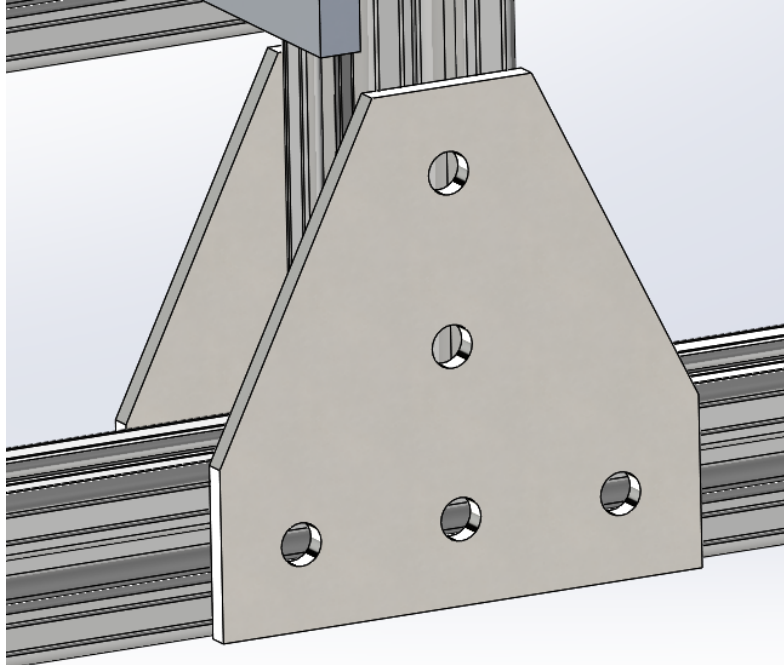
Figure 14: Bracket mounting of t-slotted bars using purchased gusset plates.

Each of the extrusions are 20" in length. A faceplate will be attached to the frame using the same fasteners as in the bracket. This faceplate will contain dowel pins and threaded holes for the purpose of mounting devices to the testing rig. To ensure proper leveling of the device, metal swivel-mounted feet will be positioned on the top and bottom of the assembly. These feet will be attached to a threaded rod which in turn is threaded through the t-slotted bar with 8-32 thread. This subassembly is then capped with a three pronged handle, allowing for fine adjustment of the leveling system (Figure 15).
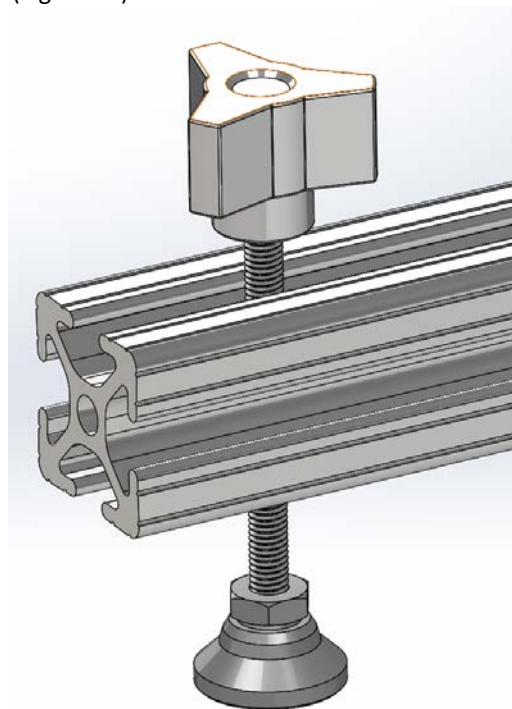

Figure 15: Leveling system comprised of swivel feet and an adjustment knob.

3.2.b Cylinder Mount Subassembly
To rigidly mount the cylinders, two 3D-printed v-block assemblies will be attached to the faceplate using dowel pins and threaded holes. We chose to 3D print these v-blocks for two reasons: first the manufacturing complexity of the blocks would make it difficult to mill, and second the ABS material reduces possible damage to the cylinders due to its soft nature. The top of the v-block is mated to the bottom via screws threaded to the faceplate, and the compression on the cylinder constrains it. Since we are using many different types of cylinders, two different sizes of v-blocks will need to be manufactured.

3.2.c Calibrated Mass Carriages
To apply forces to our cylinders, weight carriages were designed to rigidly attach to the end of the cylinder rods. These carriages will be 3D printed due to complexity and are designed to hold calibrated weights. The weights themselves have holes on the underside, so a peg on the bottom of the carriage is used to hold the weights in place. To mount the carriages to the pistons, a through-hole is cut in the top of the carriage. To accompany different rod diameters, custom washers will be bored to the proper dimension. The cylinder rod is then placed between two washers and the hole in the top of the carriage, and nuts lock the carriage in place from both sides. To accompany single-acting cylinders, a similar design is implemented but the carriage is flipped upside down, calling for a total of 4 carriages needed. Each carriage is capable of holding up to 1kg.

3.2.d Encoder Mount Subassembly
We began design of the encoder mount subassembly by determining the key functionality that it should possess, namely that it should couple the encoder's motion to the linear motion of the cylinder while minimizing frictional losses and rotational inertia. To accomplish this we looked at drawstring encoders used for linear motion tracking because of their simplicity and adaptability to different displacement ranges. We chose to incorporate this style of tracking because simply couples linear and rotational motion while remaining compact, and can quickly be adapted for different actuator strokes.

Due to budget restrictions we could not feasibly purchase two drawstring encoder assemblies, however through research we developed the knowledge to design our own custom solution. To accomplish the critical push-pull functionality of the drawstring encoder we looked to similar-type systems on the market which offer near constant, low retraction forces in a relatively compact design. Unfortunately, these systems too were relatively expensive and would require modification in order to attach an encoder.

We chose to develop a custom solution incorporating the key elements of drawstring encoders and low-force cable retraction systems into a design that could be quickly assembled onto our testing apparatus. For this there were three significant modules: the constant-torque spring motor assembly, the cable spool, and the encoder wheel and sensor. We began by designing the constant-torque spring motor that would provide the restoring force to the encoder system during push-operation. For this we chose to start with 1.81 (in-lb) nominal Neg'ator® spring motors as a first iteration. Using the supplied dimensions we then designed the output and storage drums to the manufacturer's specifications; for this we chose to use delrin for the drums to minimize their rotational inertias. After the spring motors we looked into cable spools and chose to use 1.39 (in) diameter timing pulleys our team acquired. Finally we began looking at optical encoders and chose to use a 2 (in) diameter 2048 (CPR) transmission encoder from US Digital in conjunction with the correct Encoder Module. We chose to use these encoders because using the 2 (in) diameter encoders still allowed for a compact design while allowing for 0.002 (in) linear resolution when coupled with our cable spool. We believed that the significant increase in resolution between 1024 (CPR) and 2048 (CPR) systems outweighed their marginally higher cost and so chose to use the higher resolution encoders.

Our final encoder mount subassembly compactly couples the three aforementioned modules together onto a mount that can be quickly fixed to the testing apparatus through two ¼-20 cap screws (Figure 16) and is right-hand or left-hand configurable depending on the orientation of the two drums. To change the configuration it is only necessary to switch the drums' phase 180° and re-attach the constant-torque spring (Figure 17).
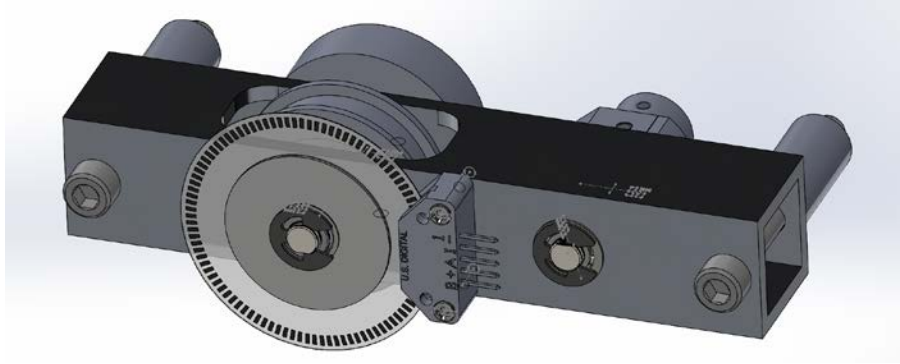
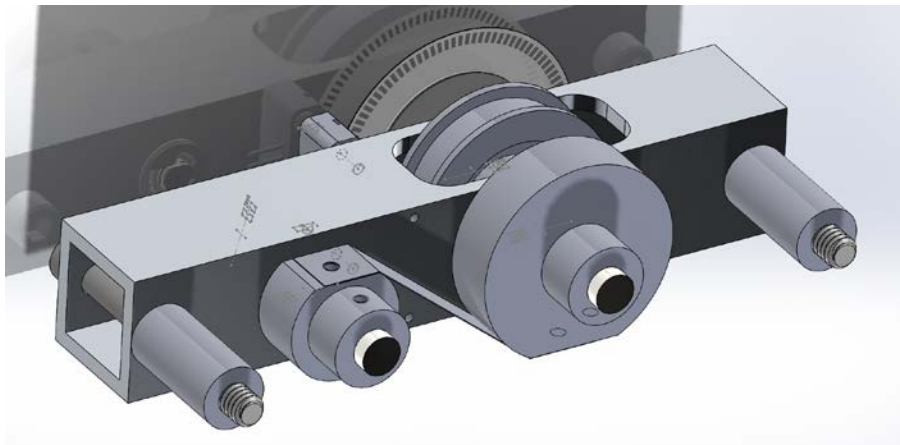Figure 16: Front view of drawstring-style encoder assembly.

Figure 17: Rear view of drawstring-style encoder assembly highlighting constant force spring and drum-spools.

After completing the design process we used the mass properties function in Solidworks 2015 to obtain the effective moment of inertia about the rotational axis of the system. Since our testing apparatus uses a constant gravity vector field we set the maximum acceleration to 9.81 (m/s^2) and then determined the required restoring torque to be 0.004 (N-m). Comparing the required torque and the spring motor torque of 1.84e-2 (N-m) we obtained a factor of safety of 56.7. Using the same moments of inertia we then calculated the effective safety factors for different available springs and chose to use a 0.035 (N-m) constant torque spring which gave us a safety factor of 9.6. While still over-engineered we chose to use this spring for ease-of-manufacture and availability.

3.2.e Testing Apparatus Pre-Pressurization and Hydraulic Bleeding System
Through running simulations we determined that pre-pressurizing of both pneumatic as well as hydraulic systems has the potential to increase the overall system efficiency and therefore decided to incorporate a pre-pressurization system into our testing apparatus. To simplify the bleeding process required for hydraulic cylinders we also designed a system comprised of valves and a reservoir and combined the two into one system. Shown in Figure 18 is a schematic depicting our valving design which allows us to bleed both ends of both double acting or single acting cylinders, in addition to pressurizing the system with an external air compressor. By changing the direction of the three-way valves between the cylinders and the reservoir we can alternately charge and bleed the cylinders and conduit lines prior to testing. Additionally, these valves allow us to isolate our testing system, the two cylinders and connection conduit, from the other elements during testing. We chose this design because it allows us to use the same pressurization process for both types of fluid actuators, while still allowing us to test hydraulic and pneumatic systems with the same hardware.
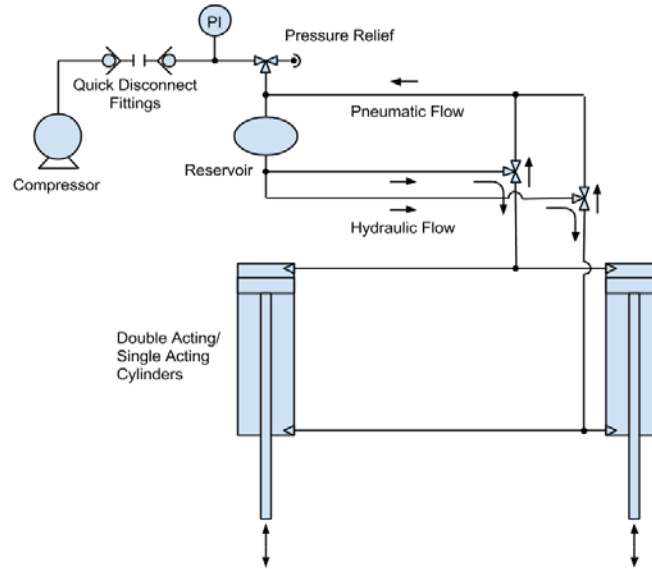
Figure 18: Pre-pressurization and hydraulic bleeding system.

3.3 Testing Methodology Development

We plan to directly compare different passive power transmission systems against each other using our testing apparatus and are currently developing the testing methodology with which we plan to conduct testing. While many model parameters such as geometry and material properties will be known prior to conducting testing, several sub-system level considerations such as Bowden cable effective stiffness, and the thermal time constant in each pneumatic cylinder must first be evaluated prior to comparing experimental results to our theoretical models. For a complete overview of our testing plan see Appendix 1.

3.3.a Bowden Cable Considerations

The major parameter a Bowden cable system that we must evaluate is the effective stiffness of the conduit and cable together. In order to do this we plan to follow the model outlined in [1] where the stiffness is directly extracted from experimental results using regression techniques. Once determining this value we can then run simulations and compare the results of our experiment and mathematical model.

3.3.b Pneumatic Model Considerations

Testing pneumatic actuators poses unique challenges over strictly testing Bowden cables because of the complicated thermodynamic-mechanical relationships occurring between the master and slave cylinders, and the environment. In order to simulate these models it will first be necessary to experimentally obtain three critical values for each cylinder, namely the average heat transfer coefficient, the static friction constant, and the coefficient of viscous damping. To obtain the average convection heat transfer coefficient we will follow an experiment similar to the one outlined in [3] where the step pressure response of a cylinder will be monitored in order to derive the thermal pressure time constant for each cylinder. Following this experiment, the static friction and coefficient of viscous damping terms will be experimentally determined using calibrated masses and gravity to apply a known force to the cylinder rod while the displacement of the system is monitored in time.

3.3.c Dynamic Efficiency Testing

The second form of testing we will be conducting is designed to compare the mechanical efficiency of Bowden cables against pneumatic and hydraulic cylinder actuators. For this we plan to only consider the input and output of the system with an energy analysis because known forces will be applied to both sides and known displacement will be tracked in time. Additionally, by comparing all systems with the same input mechanisms we hope to gain an understanding of the relative efficiencies of each under similar conditions

IV) RESULTS

The following section outlines the results we obtained through empirical testing of pneumatic and hydraulic actuators and the analysis methods used to determine efficiencies of each system. The tested conditions are outlined in Table 6. Due to time constraints, Bowden cables were not able to be tested although we still believe that a direct comparison between cable and fluid transmission systems will yield an insightful comparison and is worth undertaking.

Table 6: List of testing conditions fulfilled during empirical testing.

Cylinder Mod. #	Bore/ Stroke	Seal	Fluid	Tube Length/ Dia. (in)	Pre-Pressure (psi)	Mass Combos [Master, Slave] (g)
Airpel E16DU2	0.627"/ 2.00"	Gap	Air	30/.125	[0, 20, 30, 40]	[500, 0], [500, 200], [1000, 200], [1000, 500]
			Water	10/.125	[0, 20, 30, 40]	[500, 0], [500, 200], [1000, 200], [1000, 500]
Bimba CM-043-DXPW	0.750"/ 3.00"	Contact	Air	30/[.125, .375]	[0, 20, 30, 40]	[500, 0], [1000, 0], [1000, 200], [1000, 500]
			Water	10/.125	[0, 20, 30, 40]	[1000, 0], [1000, 200]
ControlAir 349-180-00	0.700"/ 0.70"	Diaphragm	Water	10/.125	5	[1000, 200], [1400, 200], [1400, 500]

4.1 Analysis Techniques used to Determine Experimental System Efficiency
We began analyzing the data by separating the hydraulic and pneumatic data because the experimental results showed very different trends.

4.1.a Analysis Techniques used for Pneumatic Systems
The data collected during testing the pneumatic systems compiled using Matlab 2015 and separated by trial point in order to compare repeated tests. Across all parameter variations for the same seal type, there was a similar trend with three distinct regions (Figure 19). Consisting of an at rest portion, a nearly linear velocity regime, and a post-actuation regime that differed between contact and gap seal cylinders, the similarity between datasets during actuation allowed for a uniform analysis method to be employed across all tests. We note that, despite the consistency of the trend, several test runs using Airpel E16D2.0U gap seal cylinders occurred in such a manner as to produce a skip in the encoder readings; upon settling these test runs showed negative displacement data. To account for this the steady-state resting position was taken as a DC offset and applied uniformly across the data beginning at the negative inflection point which signified the end of the stroke. This data was then analyzed in the same manner as all other datasets.
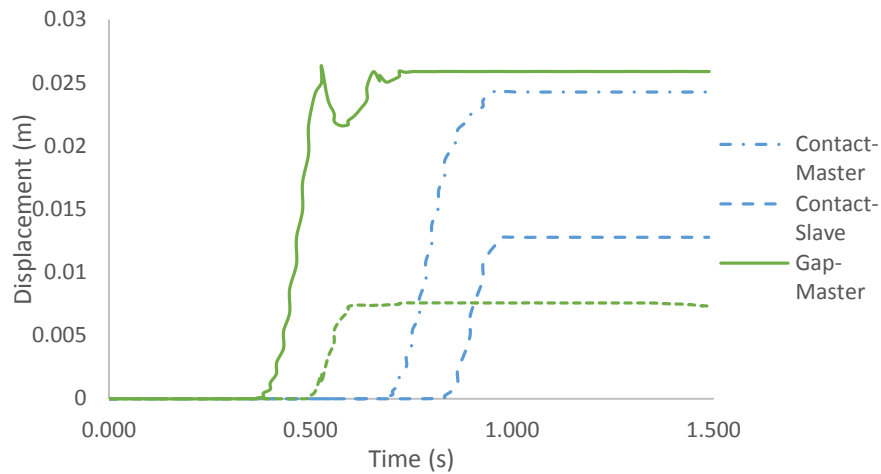

Figure 19: General trend of pneumatic test data showing the distinction between seal type. Tests are done with master-slave mass inputs of 1000 (g) and 500 (g) and at atmospheric pressure.

For each dataset a simple Boolean search algorithm was developed to identify the points where motion began and where motion ended independently for the master and slave cylinder. Using these bounding points the data between was then taken and a first order polynomial fit applied to it. Using the resulting polynomial slope as an average velocity, the resulting kinetic energy of each mass at the end of actuation was computed through the relationship shown in Equation 19. Using the final points of both strokes, the initial potential energy of the master cylinder mass and the final potential energy of the slave mass were computed through Equation 20.

$$KE = \frac{1}{2}m_i \bar{v}_i^2 \qquad (19)$$
$$PE = m_i g h_{end} \qquad (20)$$

Using our definition of system efficiency outlined in Equation 21, we then computed the system efficiency as the ratio of final system kinetic and potential energy to the initial system potential energy. Error analysis was performed as well, using the standard deviations of the polynomial fit along with the average final displacement of the masses. These terms were carried through the previous computations to arrive at a final error in efficiency.

$$\eta_{sys} = \frac{KE_1 + KE_2 + PE_2}{PE_1} \qquad (21)$$

4.1.a.i Determination of Viscous Damping Coefficient for Pneumatic Simulation
For the state-space pneumatic simulation it was necessary to determine the viscous damping coefficient for each cylinder. Using the data collected in the manner outlined in Section 3.3.b data was collected for the tested cylinders and then compiled into Microsoft Excel 2014 for analysis. Due to the high level of linearity present in the data and the low density of data-points we began by applying a linear fit to the actuation portion of the stroke in order to determine an average velocity. Since both chambers were open to atmospheric pressure, we neglected any pressure differential between them, and solved Equation 22 for the steady state friction force. Assuming these conditions, the viscous damping coefficient for each cylinder was then extracted using the previously computed velocity.

$$F_{friction} = \bar{v}b = mg \qquad (22)$$

4.1.a.ii Determination of Thermal Time Constant for Pneumatic Simulation
Arising from the limitations of our testing apparatus, we were unable to collect sufficiently clean data with which to analyze the thermal time constants of the pneumatic cylinders. Despite this setback, we ran simulations using varying orders of magnitude for the average heat transfer coefficient under our tested operating conditions, and determined that the heat transfer did not have adequate time to develop a substantial impact. For a complete overview of the pneumatic system simulations compiled see Appendix 3.

4.1.b Analysis Techniques used for Hydraulic Systems
The efficiency number that we sought to calculate was defined as the ratio of the input and output work of the system. To determine the value of these quantities, it was necessary to identify the forces acting at both the input and output of the transmission and the velocities at which they acted. To begin the analysis for the hydraulic system, tab delimited data was read into Microsoft Excel 2014. There, the timestamps were processed to give the time elapsed in seconds and the encoder counts were converted to linear displacement using the geometric properties of the encoder assembly through Equation 23.

$$x_n = \frac{d\pi N}{res} \qquad (23)$$

The prepared data was then imported into Matlab R2014a for further processing. In order to be able to differentiate the time-series position data, it first had to be smoothed to remove any artifacts of the data acquisition process. Attempting to differentiate the raw data would yield useless results, as any noise in the original data would be amplified. The data was processed using a localized regression algorithm, LOESS, after

which the velocity and acceleration profiles were approximated through an implementation of a central finite difference method defined in Equations 24 and 25.

$$\left(\frac{dx}{dt}\right)_i \cong \frac{x_{i+1}-x_{xi-1}}{t_{i+1}-t_{i-1}} \tag{24}$$

$$\left(\frac{d^2x}{dt^2}\right)_i \cong \frac{x_{i+1}(t_i-t_{i+1})+x_{i-1}(t_{i+1}-t_i)-x_i(t_{i+1}-t_{i-1})}{\frac{1}{2}(t_{i+1}-t_{i-1})(t_{i+1}-t_i)(t_i-t_{i-1})} \tag{25}$$

To simplify the analysis, the loads at either end of the transmission were considered to be lump masses, consisting of the piston/rod assembly, the mass carriage, and whichever calibrated masses were loaded into the carriage. Knowing these masses, the velocity and acceleration of the loads over time, and the external influence of gravity, we have everything necessary to calculate the powers.

The net force on the driving mass, m_1, is the product of the mass and its acceleration, $F_{1,net}=m_1a_1$. The external force exerted on the mass by gravity is $F_{1,g} = m_1g$. Therefore, the force input to the transmission is $F_{in}=m_1(g - a_1)$ and the input power is $P_{in} = m_1v_1(g - a_1)$. On the other side of the transmission, the driven mass has a net force of $F_{2,net}=m_2a_2$ acting on it. Since this net force is in the opposite direction of gravity's influence, the magnitude of the force exerted on the driven mass by the transmission must equal the sum of those forces, $F_{out}=m_2(g + a_2)$. Therefore, the output power of the transmission is $P_{out}=m_2v_2(g + a_2)$. Integrating the power terms with respect to time yields the input and output work terms, which can then then be used to calculate the desired efficiency value.

The theoretical model equations were evaluated in Wolfram Mathematica 10 at each set of test conditions to obtain expressions for conduit and cylinder efficiency as functions of piston velocity. The appropriate functions were applied to each velocity profile in Matlab, with the master and slave cylinders in each data set being evaluated separately. The overall system efficiency was then calculated as the product of the component efficiencies using Equation 26.

$$\eta_{sys} = \eta_{cyl_1}\eta_{cyl_2}\eta_{conduit}^2 \tag{26}$$

The time average of this theoretical efficiency was taken using trapezoidal integration in Matlab and then dividing the result by the time span. Averaging gives a value that can be directly compared with the experimentally determined efficiency value for each trial.

4.2 Effect of Tested Parameters on Pneumatic System Efficiency
Through our testing we parametrized seal type, conduit diameter, input masses, and pre-pressurization with pneumatic actuators, and compared their relative influence on system efficiency. The following section details each specific parameter's impact on overall efficiency.

4.2.a Effect of Seal-Type on Efficiency
Different piston sealing designs contribute differently to the overall system dynamics, and each have inherent tradeoffs associated. The static friction found inherent in the contact seal cylinders we tested was significantly larger than that found in the gap style seals, lending itself to lower simulated system efficiencies for the same given input parameters (Fig. 20). Figure 20 compares the simulated and tested system efficiencies for both seal types across different pre-pressurizations, and while the general trend is consistent, the experimental data shows a different trend between seal types than does the simulated data. From our experiments the contact seal cylinders produced higher efficiency data-sets than the gap seal cylinders over all testing conditions an average of 11.8 ± 1.5 (% Efficiency).
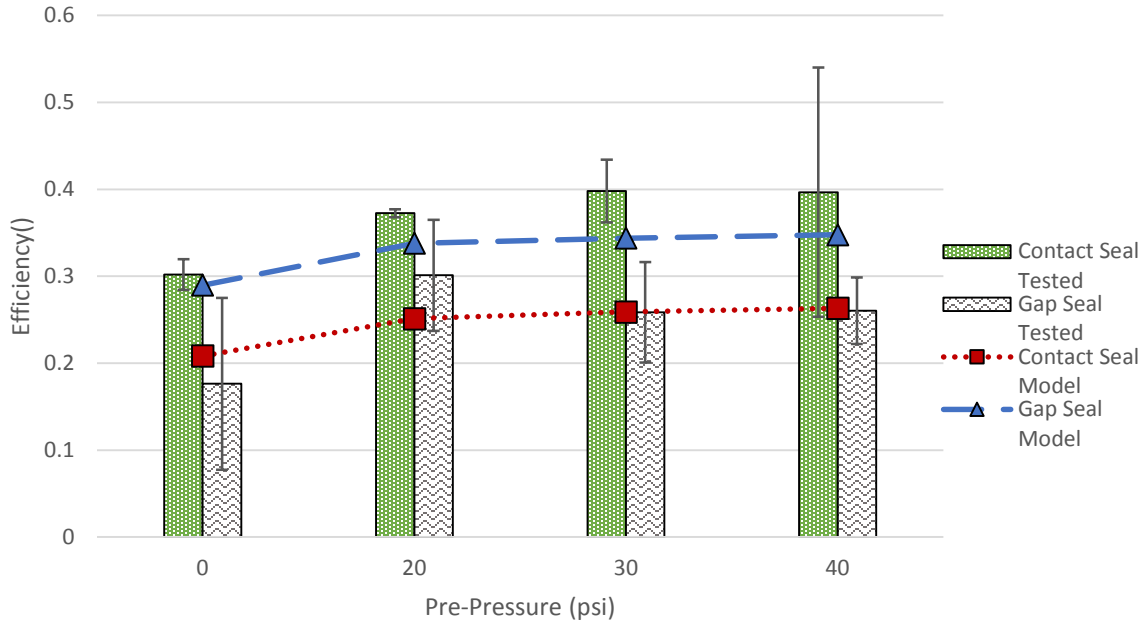
Figure 20: Effect of seal-type on pneumatic system efficiency across pre-pressurization for 1/8" conduit diameter, and master-slave masses of 1000 (g) and 500 (g) respectively.

4.2.b Effect of Conduit Diameter on System Efficiency

Conduit diameter too plays a role in the overall pneumatic system efficiency through both viscous flow losses, and geometrically in the form of latent compressive volume and additional heat transfer surface area. Figure 21 compares the simulated and experimentally derived efficiencies between conduit diameters across different pre-pressurizations using contact seal cylinders. While both sets of experimental data show efficiencies higher than the predicted simulation, the trend remains consistent across the range of pre-pressurizations. Further investigation into this phenomenon in order to quantify its source.
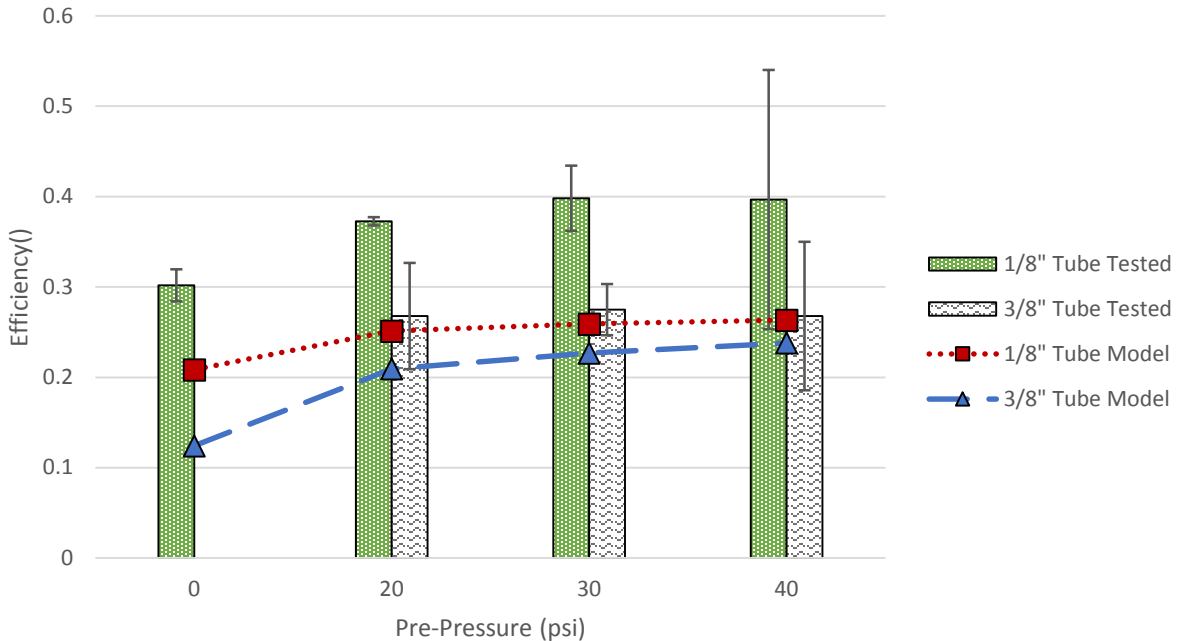

Figure 21: Effect of conduit diameter on pneumatic system efficiency across pre-pressurization using a contact-type seal and master-slave masses of 1000 (g) and 500 (g) respectively.

4.2.c Effect of Mass on System Efficiency
During testing and through data analysis we noticed that the system response improved when the applied masses were increased, additionally, the system response improved when the slave cylinder mass was increased. The general trend observed in both experimental data and simulation results shows that within our tested mass configurations, efficiency increases as the ratio of output mass to input mass increases (Fig. 22).
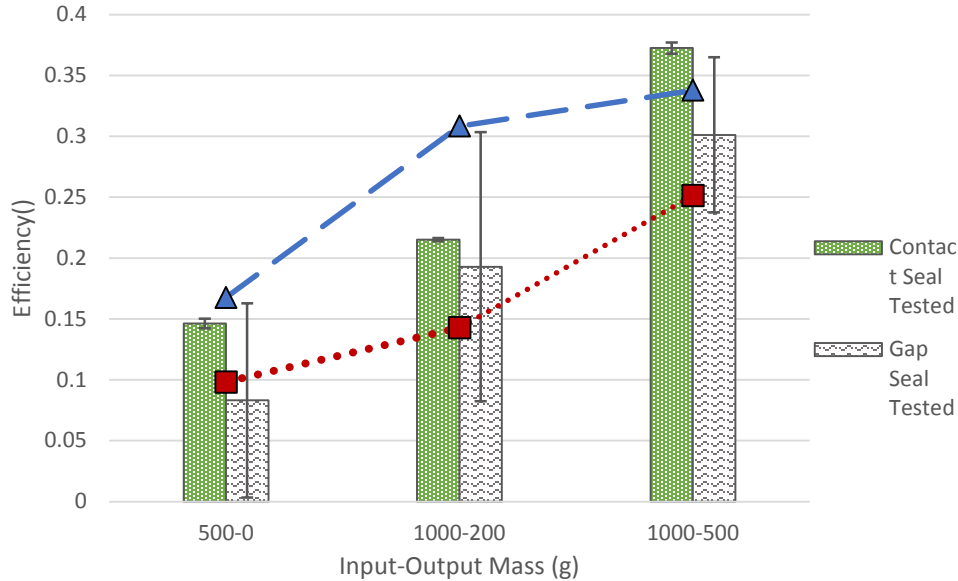

Figure 22: Effect of input and output masses on pneumatic system efficiency for 1/8" conduit diameter and a pre-pressurization of 20 (psi).

4.2.d Effect of Pre-Pressurization on Efficiency
Pre-pressurizing the system shows an upward trend in theoretical system efficiency for both pneumatic and hydraulic systems. In pneumatic systems, pre-pressurizing the system works in a similar fashion to a pre-loaded spring, where the stiffness of the system is increased in order to increase the system's effective power transfer.

4.3 Effect of Tested Parameters on Hydraulic System Efficiency

4.3.a Effect of Mass on Efficiency
In our testing, we found a significant relationship between the mass difference and the resulting system efficiency. Figure 23 shows the experimental efficiency of the rolling diaphragm cylinders for various mass configurations, ordered by input/output mass ratio. On the low end, we see that a mass ratio of 20:1 results in an efficiency of 0.168 ± 0.044. As the mass ratio decreases to 2.5:1, we see that efficiency increases to 0.371 ± 0.024. The same relationship existed for the other cylinder types, with efficiency increases as load-matching was improved. As the volumetric efficiency of the cylinders is very high in hydraulic use, we believe this result is due to us not making use of the system's full potential for power transmission.
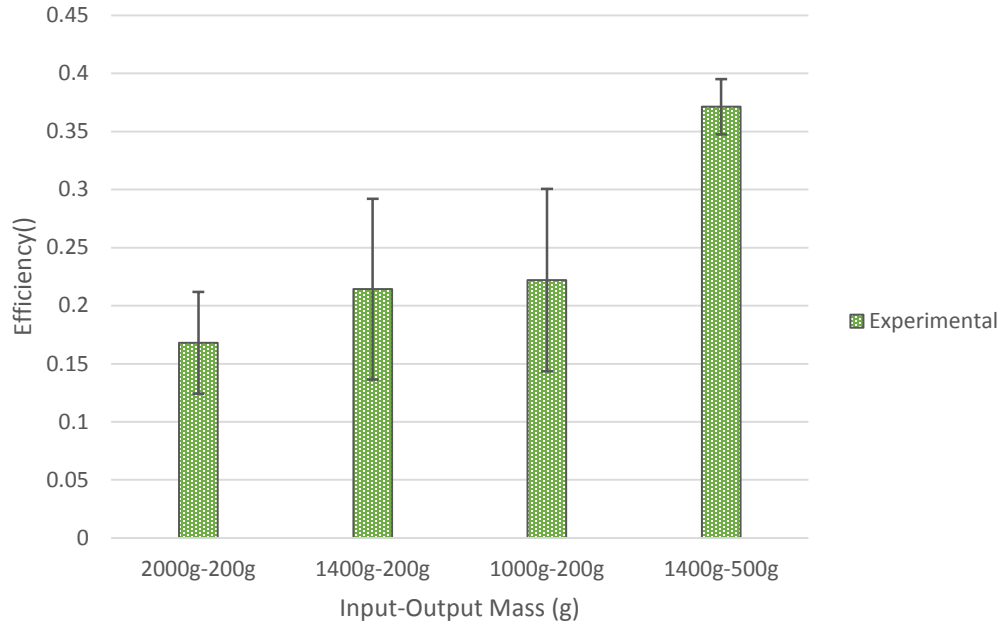
Figure 23: Effect of input and output masses on hydraulic system efficiency using rolling diaphragm cylinders at atmospheric pressure.

4.3.b Effect of Seal Type on Efficiency

Due to the aforementioned issues with the load-balancing affecting the experimental efficiency values, we cannot appropriately evaluate the force efficiency. However, by looking at the displacement profiles of the different cylinder types operating under the same conditions, we are able to compare their volumetric efficiencies. Figure 24 shows two such profiles, with the contact seal cylinder demonstrating a much higher volumetric efficiency than the gap seal cylinder. The contact seal cylinder also appears to have a much shorter delay between the actuation of the master cylinder and the response of the slave cylinder.
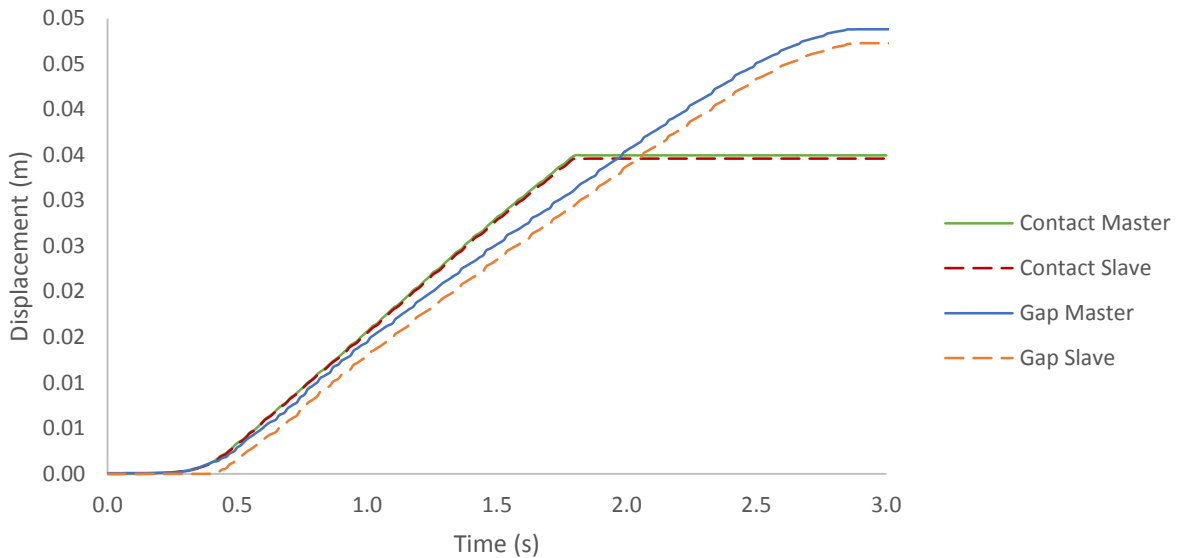

Figure 24: Displacement profiles of contact and gap seal cylinders in the hydraulic system. Tests were run using a master-slave mass configuration of 1000 (g) and 200 (g), at a pre-pressurization of 20 (psi).

25

V) DISCUSSION

Although some trends agree with the simulated systems, there still exist issues and aspects of uncertainty within the testing system that require refinement or quantification.

5.1 Closeness of Experimental and Simulation Results

In comparing the simulation and experimental results several things became clear. Generally speaking, the simulated pneumatic system predicts lower efficiency than we computed from the experimental data. Several things may be driving this, however we believe that the largest contributing factor is an incomplete understanding of the losses within the system (thermodynamic, and mechanical). We believe that this incomplete understanding has led to incorrect assumption such as a uniform viscous damping coefficient, which may be artificially depressing the simulated efficiency values. Despite this, however, the experimental gap-seal efficiency values were lower than the simulated system which we believe to be directly related to the sampling-rate issues our data acquisition system was having during the quick actuation period.

In essentially all of our tested hydraulic cases, the experimental data did not line up with our mathematical model which we attribute to the high volumetric efficiency of hydraulic systems. To this point, we believe that we may have been operating the system sub-optimally through ineffective loading.

5.2 Critique of Testing Apparatus Design

Beginning with the pressurization system, the testing apparatus has several features that require modification or re-design in order to minimize the level of uncertainty. . While largely leak-free, the gauge chosen has leaks within the gauge body itself. This issue was resolved by closing the first three-way valve after pressurization, but in order to obtain an accurate pressure reading the compressor must remain attached. The mass carriages worked as intended, however they were limited in the range of masses that could be applied, and the 3D printed material limited the maximum mass that could be attached.

5.3 Sources of Experimental Error

Several sources of experimental error arise from unknowns within the testing apparatus, all of which may be fixed and/or quantified with further attention. Our data acquisition system uses a string wound pulley to measure displacement that is then attached to the bottom of the weight carriage via a hook. During actuation these strings are not perfectly vertical to the cylinders, leading to marginal inaccuracies in the displacement readings. While small, these slightly off axis loads may impact the dynamics of cylinder movement due to increased friction. To solve this, the encoder assembly can be mounted further into the faceplate to achieve proper clearance for all cylinder types. Additionally, these pulleys are tensioned using constant torque springs which have a rated linearity of $\pm$ 10% throughout their full-scale range which may be quantified but is unknown at this time, and therefore adds uncertainty to the exact force input on each piston-rod. . Finally, the data acquisition system showed resolution errors that impacted the data collection process during pneumatic testing. Since the Arduino chosen for data acquisition runs on interrupts, it is unable to keep up with the recording speed of the encoder, leading to Skipped data points during fast actuation.

5.4 Future Work

Due to the sheer number of permutations, further testing should be performed in order to validate the models. Only three different cylinders were tested, with the intention of determining the contribution that seal-type has on system efficiency. Further data collection can be done on cylinders with different bore sizes and stroke lengths. Along with this, data should be taken using the 1/4" tubing, since current testing has only been done using 1/8" and 3/8" tubing,. In order to determine how much the viscosity of the fluid impacts efficiency, tests should be run using additional fluids such as isopropyl alcohol, with higher and lower viscosities than water.

Along with further data acquisition, new testing methods should be established to obtain different sets of data. If our system was attached to a DC-driven servomotor, constant velocities could be applied to the driving cylinder. This movement would be more representative of a patient's movement, could provide a larger range of time in which to collect data, and gives a higher level of control over the input into the system. Furthermore, the cylinders tested showed a strong correlation with mass input, and the models show strong efficiency correlation with

actuation velocity. Running tests using controlled sinusoidal inputs could provide much higher efficiencies than established by our trials using a free fall method, and would have the added benefit of developing a frequency response.

VI) ACKNOWLEDGEMENTS

SOURCES
[1] Agrawal, V., Peine, W., Yao, B., 2010, "Modeling of Transmission Characteristics Across a Cable-Conduit System", *IEEE Transactions on Robotics, Vol 26 No-5.*
[2] Andrighetto, P., Valdiero, A., Carlotto, L., 2006, "Study of the friction behavior in industrial pneumatic actuators", *ABCM Symposium Series in Mechatronics, Vol 2 pp. 369-376.*
[3] Carneiro, J., Almeida, F., 2006, "Heat transfer evaluation of industrial pneumatic cylinders", *Department of Mechanical Engineering University of Porto Portugal.*
[4] Els, P., Grobbelaar, G., 1999, "Heat transfer effects on hydropneumatic suspension systems", *Journal of Terramechanics, Vol 36 pp197-205.*
[5] Juvinall, Robert C., 1961, "Gas-Liquid Pressure Transmitter", *Department of Physical Medicine and Rehabilitation Orthetics Research Group, pp. 10-26.*
[6] Katzschmann R., Marchese A., Rus D., "Hydraulic Autonomous Soft Robotic Fish for 3D Swimming", *MIT Computer Science and Artificial Intelligence Laboratory Cambridge MA.*
[7] Maciejasz P., Eschwiler J., Hahn K., Troy A., Leonhardt S., 2014, "A survey on robotic devices for upper limb rehabilitation", *Journal of NeuroEngineering and Rehabilitation,*
http://www.jneuroengrehab.com/content/pdf/1743-0003-11-3.pdf
[8] Pinedo S. et al., 2014 "Rehabilitation efficiency and destination on discharge after stroke", *European Journal of Physical and Rehabilitation Medicine, Vol 50 No-3.*
[9] Pylatiuk C., Kargov A., Gaiser I., Werner T., Schulz S., Bretthauer G., 2009, "Design of a Flexible Fluidic Actuation System for a Hybrid Elbow Orthosis", *IEEE 11th International Conference on Rehabilitation Robotics.*
[10] Roth, E.J., 2009, "Trends in stroke rehabilitation", *European Journal of Physical and Rehabilitation Medicine, Vol 45 No-2.*
[11] Stein, J., 2009, "Adopting new technologies in stroke rehabilitation: the influence of the US health care system", *European Journal of Physical and Rehabilitation Medicine, Vol 45 No-2.*
[12] Whitney J., Glisson M., Brockmeyer E., Hodgins J., 2014, "A Low-Friction Passive Fluid Transmission and Fluid-Tendon Soft Actuator", *Disney Research Pittsburgh PA.*
[13] Xia Jicheng, Durfee William K. Analysis of Small-Scale Hydraulic Actuation Systems J. Mech. Des. **135**(9), 091001 (2013) (11 pages)
[14] Xia Jicheng, Durfee William K., 2011, "Modeling of Tiny Hydraulic Cylinders", *52nd National Conference of Fluid Power*, Paper Number 25.3, pp. 1-5

Authors

Bryan Boyer - *Mechanical Engineering '15*
Born and raised in Livonia, Michigan Bryan spent most of his early years with Lego and other construction toys which helped fuel his love for engineering. His love for science and curiosity about everything around him drove his imagination and crafted him to become the person he is today. In his free time Bryan enjoys hobbies such as archery, euchre, tennis and soccer. His hopes for the future include moving into the field of mechatronics and robotics and to one day build his own butler.

Rob Shone - *Mechanical Engineering '15*
Born in October of 1992, Rob spent his childhood growing up outside of Rochester, New York. His interest in engineering was noticed at an early age as he took apart every toy his parents gave him, with LEGOs proving to be a valuable remedy to this problem. Growing up in the second snowiest city in America, he thinks Michigan winters are mild. He is also known to be hyper-competitive: it is not uncommon to see some rock paper scissors games go to best 25 out of 49. In his free time Rob enjoys playing soccer, golf, and tennis; and during the winter is an avid skier. Currently, he has a high interest in wearable technology, prosthetics, and entrepreneurship.

Nicholas Skriba - *Mechanical Engineering '15*
Growing up in Northern Michigan, Nick is a very avid outdoorsman and enjoys hunting, fishing, gardening, and going to any one of Leelanau County's many beaches. As a kid, Nick too enjoyed playing with LEGOs and drawing pictures of buildings; and before pursuing engineering, he very seriously considered Architecture. In his free time Nick studied and helped to teach the kid's taekwondo classes before moving to Ann Arbor, where his free time has been largely spent playing music and cooking. Before transferring to the University of Michigan, Nick spent three years at NMC community college in Traverse City where he worked as a line-cook and finished his Associates Degree. He still enjoys working with his hands and building things whenever possible and has a growing interest in advanced machining systems, robotics, and optics.

David Stewart - *Mechanical Engineering '15*
Born in February 1993, David grew up in Toledo, Ohio. When he was young, he spent a lot of time building and disassembling things with LEGO and K'NEX, with his siblings providing a source of creative competition. David originally had intended to study mathematics in college, but engineering drew him in instead, with its more practical application of math principles. David is a member of the Michigan Pi Rho chapter of Pi Tau Sigma and frequently tutors friends, classmates, and siblings. In his free time, he enjoys bicycling, video games, discovering new music, and playing Euchre with friends and family. In the fall, David plans to return to the University of Michigan to pursue a Masters Degree in Mechanical Engineering, with his studies focusing on fluid mechanics and the use of CFD modeling software.